

“Spectral Implementation” for creating a labeled pseudo-pure state and Bernstein-Vazirani's algorithm in a four-qubit NMR quantum processor

Xinhua Peng^{1*}, Xiwen Zhu¹, Ximing Fang^{1,2}, Mang Feng¹, Kelin Gao¹, and Maili Liu¹

¹*Laboratory of Magnetic Resonance And Molecular Physics,
Wuhan Institute of Physics and Mathematics, the Chinese Academy of Sciences,
Wuhan, 430071, People's Republic of China*

²*Department of Physics, Hunan Normal University, Changsha, 410081, China*

ABSTRACT

A model of quantum circuit is introduced to describe the preparation of a labeled pseudo-pure state by multiplet-component excitation scheme and has been experimentally realized on a 4-qubit nuclear magnetic resonance quantum processor. Meanwhile, we theoretically analyze and numerically investigate a low-power selective single-pulse implementation of a controlled-rotation gate, which manifests its validity in our experiment. Based on the labeled pseudo-pure state prepared, a 3-qubit Bernstein-Vazirani's algorithm has been experimentally demonstrated by spectral implementation. That is, the “answers” of the computations are identified from the split peak positions in the spectra of the observer spin, which are equivalent to projective measurements required by the algorithms.

* E-mail: xhpeng@wipm.ac.cn and xinhuapeng555@hotmail.com ; Fax: 0086-27-87199291; Tel: 0086-27-87197740.

I. INTRODUCTION

Quantum mechanics provides a novel way to process information that extends the extraordinary capabilities of a quantum processor beyond those available on a classical physical system [1-4]. It is found that certain intractable problems to classical computers can be efficiently solved on quantum computers. A variety of quantum algorithms have been developed recently, e.g., the most notably Shor's quantum factoring algorithm [5] with the *exponential* speedup over classical ones. Besides, an important class of quantum algorithms is to solve the problems of analyzing the contents of a “black box” *oracle* that performs *a priori* unknown unitary transformation faster than the best classical algorithms, in despite of a “relativized” exponential speedup [6]. These algorithms include Grover's search algorithm [7], Deutsch's algorithm [8], Deutsch-Jozsa algorithm [9], Simon's algorithm [10] and Bernstein-Vazirani's algorithm [11] etc. Hitherto, many possible approaches have been proposed for the physical implementation of quantum computers [4]. Of these methods, liquid-state nuclear magnetic resonance (NMR) is arguably the most successful one [12] and has established small (up to 7 quantum bits) but fully operational quantum processors [13]. Although there are a few practical and theoretical limitations on its scalability, the experience of implementing liquid-state NMR quantum computation may be useful to build up a robust and practical quantum computer. The recent research showed that NMR techniques have been successfully applied to ion trap quantum computing [14].

Different from the usual scheme of energy-level implementation, Madi et al. proposed “spectral implementation of a quantum computer” [15] by employing an additional observer spin I_0 that is coupled to the spins carrying n computational quantum bits (qubits) I_1, I_2, \dots, I_n , which allows a mapping of the states of a quantum computer on a set of transitions between energy levels. Concretely, 2^n logic states of an n -qubit quantum computer are assigned to 2^n individual spectral resonance lines of spin I_0 , each of which can be conveniently represented by the operators in spin Liouville space

$$I_{0x} I_1^{\alpha/\beta} I_2^{\alpha/\beta} \dots I_n^{\alpha/\beta}, \quad (1)$$

where $I_i^\alpha = |0\rangle_{ii}\langle 0| = \frac{1}{2}(E_i + 2I_{iz})$, $I_i^\beta = |1\rangle_{ii}\langle 1| = \frac{1}{2}(E_i - 2I_{iz})$, $I_i^\alpha + I_i^\beta = E_i$ (the 2×2 unit matrix), $2I_{i\eta} = \sigma_{i\eta}$ ($\eta = x, y, z$) is Pauli operators and subscript i denotes the i th spin. Each of the qubits I_1, I_2, \dots, I_n is either in the state $|0\rangle$ or $|1\rangle$. Assuming that spin I_0 has resolved scalar J couplings to all other n qubits, all logic states of the n -qubit quantum computer are distinguishable due to the nondegenerate single-quantum transition of spin I_0 . Hence, instead of a standard pseudo-pure state (PPS) with deviation $I_1^\alpha I_2^\alpha \dots I_n^\alpha$ on n

spin-1/2 nuclei, one can prepare a so-called “labeled” PPS with deviation $I_{0z}I_1^\alpha I_2^\alpha \dots I_n^\alpha$ on $n+1$ spins by employing an additional observer spin I_0 as an initial state of computation. After a single spin-selective pulse $\left(\frac{\pi}{2}\right)_y^0$, a labeled PPS is transferred to one of Eq. (1), which is easily recognizable in a NMR spectrum of spin I_0 , i.e., only one of the peaks labeled by the logic state $|00\dots 0\rangle$ is visible. An algorithmic benchmark for quantum information processing has been demonstrated in a liquid state NMR system by creating such a labeled PPS [16,17]. Moreover, the labeled PPS can be used in error-correcting codes [18]. As the final answer of a computation is possibly achieved by only detecting the observer spin I_0 , “spectral implementation” scheme of a quantum computer provides another way to read out the answers of certain computational problems, such as the database search algorithms and appears advantageous compared to a mapping on the energy levels themselves[15].

In this paper, we introduce the basic operators of quantum computation (quantum logic gates) to describe Madi's multiplet-component excitation scheme of creating a labeled PPS [15] and have experimentally initialized a NMR ensemble into a 3-qubit labeled PPS by using a 4-spin sample with one being an observer spin. By considering the exact effective Hamiltonian in a rotating frame for a low-power radio-frequency (RF) pulse on a single multiplet-component in certain weak-coupled spin system, we theoretically analyze that a multi-qubit controlled-rotation gate can be approximately obtained up to conditional phases factors whenever the RF field power is low compared to the spin-spin coupling. The gate fidelities are numerically simulated for different rotating angles and RF field powers on the 3-spin and 4-spin systems, which theoretically verifies the feasibility of implementing a single-pulse quantum controlled-rotating gate by a suitable choice of the RF field power. Furthermore, a 3-qubit quantum algorithm to solve Bernstein-Vazirani's problem has been experimentally investigated on such a NMR quantum processor. The reading-out step consists of a single spin-selective pulse followed by acquisition of the signal. The answer of the computation is encoded in the amplitudes and signs of various multiplet components in the spectrum of the observer spin.

II. CREATION OF A LABELED PSEUDO-PURE STATE

The preparation of a proper initial state is one of the most important requirements for a useful computation. Starting from thermal equilibrium, many methods have been proposed and implemented for preparing standard pseudo-pure states in NMR, including spatial averaging [19-21], temporal averaging [22,23] and logical labeling

[24-26]. For preparing such a labeled PPS $I_{0z}I_1^\alpha I_2^\alpha \dots I_n^\alpha$, several methods have also been proposed such as Madi's multiplet-component excitation scheme [15], the cat-state benchmark [16], spatially encoding [27] and the general spatially averaging [28]. Here, we introduce a basis quantum circuit to describe Madi's multiplet-component excitation scheme, which extends the preparation procedure to a more universal concept.

A. Quantum Circuit of Creating a Labeled PPS

Consider a system with $n+1$ spins $I = 1/2$ (for both a homonuclear and hetero-nuclear system), whose deviation density matrix of thermal equilibrium under the high temperature approximation can be written as:

$$\rho_{eq} = \sum_{i=0}^{2^{n+1}-1} \omega_i I_{iz} \quad (2)$$

with ω_i being the Larmor frequency of spin I_i . The state $I_{0z}I_1^\alpha I_2^\alpha \dots I_n^\alpha$ can be achieved from thermal equilibrium ρ_{eq} by applying a nonselective $(\pi/2)_y$ pulse on $n+1$ spins and a line-selective $(\pi/2)_{-y}^k$ pulse on a single multiplet line of spin I_0 , for example, on the transition where all spins I_1, I_2, \dots, I_n are in their $|0\rangle$ states, followed by a pulsed-field gradient (PFG) [15]. Any of the other states $I_{0z}I_1^{\alpha/\beta} I_2^{\alpha/\beta} \dots I_n^{\alpha/\beta}$ can be analogously prepared by irradiating a different single transition.

As RF pulses and delays in NMR actually correspond to the basic unitary operations in quantum computing [30], a universal quantum circuit is used to describe the preparation procedure of a labeled PPS $I_{0z}I_1^{\alpha/\beta} I_2^{\alpha/\beta} \dots I_n^{\alpha/\beta}$, instead of the specific pulse sequence in NMR. Before applying the final PFG, the quantum circuit to prepare a labeled PPS $I_{0z}I_1^\alpha I_2^\alpha \dots I_n^\alpha$ is shown in Fig. 1(a), consisting of $n+1$ single-qubit rotations and a controlled- R_{0y} gate that performs the operation R_y on spin I_0 if all the states of n controlling qubits are in $|0\rangle$. $R_{iy} = e^{-iI_{iy}\pi/2}$ representing a $\pi/2$ rotation along y-axis on spin I_i and R_{iy}^\dagger is its conjugated operator. The controlled- $R_{0y}(\alpha)$ gate can be expressed as a propagator

$$U_{control}(\alpha) = e^{-i\alpha I_{0y} I_1^\alpha I_2^\alpha \dots I_n^\alpha} = \begin{pmatrix} \cos(\alpha/2) & -\sin(\alpha/2) & & & \\ \sin(\alpha/2) & \cos(\alpha/2) & & & \\ \hline & & 1 & & \\ & & & \ddots & \\ & & & & 1 \end{pmatrix}. \quad (3)$$

Thus the quantum circuit in Fig 1(a) yields such a unitary propagator $U = R_{0y}^\dagger U_{control}(\pi/2) \prod_{i=1}^n R_{iy}$ that can

transform thermal equilibrium ρ_{eq} of Eq. (2) into the output state $\rho_f = U\rho_{eq}U^\dagger$. The simple calculation obtains that after a consequent PFG to eliminate all off-diagonal elements of ρ_f , the remaining diagonal matrix is just equivalence to a labeled PPS $I_{0z}I_1^\alpha I_2^\alpha \dots I_n^\alpha$ since no zero-quantum transition is generated in the procedure. Thus we initialized the computational qubits into the pure state $I_1^\alpha I_2^\alpha \dots I_n^\alpha$. Note that the state $I_{0z}I_1^\alpha I_2^\alpha \dots I_n^\alpha$ is a truly mixed state, which is the tensor product of the observer spin operator I_{0z} and the pure state $I_1^\alpha I_2^\alpha \dots I_n^\alpha$. Each state of $I_{0z}I_1^{\alpha/\beta} I_2^{\alpha/\beta} \dots I_n^{\alpha/\beta}$ can be simply obtained by modifying the state of the controlling qubits in the controlled- R_{0y} gate corresponding to the pure state $I_1^{\alpha/\beta} I_2^{\alpha/\beta} \dots I_n^{\alpha/\beta}$. For example, in order to prepare the $I_{0z}I_1^\alpha I_2^\beta I_3^\beta$ state, the value of the control string in the quantum circuit should be $|0\rangle_1|1\rangle_2|1\rangle_3$. This can be in fact achieved by conjugating the controlled- R_{0y} gate with NOT gates [6], i.e., to sandwich the controlled- R_{0y} gate between two NOT gates applied on those qubits that is in the I_i^β state in the desired labeled PPS.

Quantum circuit is an efficient and powerful model for describing quantum computation. The quantum circuit in Fig.1 (a) can be effectively implemented by using a set of universal logic gates [4]. The universal logic gates are straightforward to implement in NMR[30]. In particular, conventional NMR spectroscopy techniques provide a more natural way to implement directly some multi-qubit logic gates, such as a kind of crucial quantum controlled-operations in quantum computing. For instance, when the molecule chosen in the experiment displays resolved J couplings, due to no delays and refocusing schemes [31], the direct implementation of multi-qubit controlled-rotation gates by transition- selective pulses is simpler than that by standard J coupling gates sandwiched between spin-selective pulses [30,32] The experimental pulse sequence is shown in Fig. 1(b), inserting another PFG before the transition-selective pulse by taking account of the fast transverse relaxation effect during the low-power, long-duration transition-selective excitation.

B. Experimental Demonstration and Analyses

The physical system to demonstrate the above procedure is selected as the carbon-13 labeled alanine $NH_3^+ - C^\alpha H(C^\beta H_2) - C' O_2^-$ dissolved in D_2O and operated on a Bruker ARX500 spectrometer with respect to transmitter frequencies of 500.13 MHz for 1H and 125.77 MHz for ^{13}C . The measured NMR parameters are listed in Table 1. Due to its resolved scalar J couplings to all other spins, C^α is chosen as the observer spin I_0 . C' , C^β and H being directly joined with C^α are spin I_1 , I_2 and I_3 , respectively. The methyl protons were

decoupled during all experiments.

The transition-selective $\pi/2$ pulse on spin I_0 used to realize the controlled- R_{0y} gate in our experiment was *Gaussian* in shape and of $80ms$ duration in order to achieve sufficient selectivity in the frequency domain without disturbing the nearest line. As the low-power transition-selective excitation is, however, only an approximation of achieving the propagator of Eq. (3) and involves inevitably unwanted evolution under the internal Hamiltonian, the whole Hamiltonian of the system should be considered to predict more precise details of the spin's evolution. Accordingly, we will first show the validity of a single transition-selective pulse to implement the controlled- R_{0y} gate by analyzing theoretically the full dynamics of the excitation [29] before presenting the experimental result.

In the weak coupling limit, $2\pi J_{ij} \ll |\omega_i - \omega_j|$, the internal Hamiltonian of arbitrary $n+1$ -spin system in a large static magnetic field can be expressed as [29]

$$H_{\text{int}} = -\sum_{i=0}^n \omega_i I_{iz} + 2\pi \sum_{i<j}^n \sum_{i=0}^n J_{ij} I_{iz} I_{jz}, \quad (4)$$

where J_{ij} is the coupling constant between spins i and j . The external Hamiltonian for the applied RF field with the amplitude B_1 has the form

$$H_{\text{ext}} = \sum_{i=0}^n e^{-i(\omega_{rf}t+\phi)} \Omega_i I_{ix} e^{i(\omega_{rf}t+\phi)}, \quad (5)$$

where ω_{rf} is the transmitter's angular frequency, ϕ the initial phase and $\Omega_i = \gamma_i B_1$ the Rabi frequencies controlled experimentally by adjusting the RF power. For simplicity, assuming that the amplitude B_1 of the applied RF field is constant over the duration of the pulse, without considering the relaxation effects, the total Hamiltonian $H = H_{\text{int}} + H_{\text{ext}}$, whose time-dependence can be removed by transforming into a new frame rotating at the frequency ω_{rf} . The time-independent effective Hamiltonian in the new rotating frame [29] is then given by

$$H_{\text{eff}} = \sum_{i=0}^n (\omega_{rf} - \omega_i) I_{iz} + 2\pi \sum_{i<j}^n \sum_{i=0}^n J_{ij} I_{iz} I_{jz} + \sum_{i=0}^n \Omega_i I_{iy}. \quad (6)$$

In Eq. (6), ϕ is taken to be $\pi/2$ in order to achieve directly the controlled- $R_{0y}(\theta)$ gate. If

$\omega_{rf} = \omega_0 - \pi \sum_{k=1}^n J_{0k}$ matches the $|000..0\rangle \leftrightarrow |100...0\rangle$ transition of the multiplet components of spin I_0 , it

is shown in Appendix A that if $|\Omega_0| \ll 2\pi |\min(J_{0i})|$, the full evolution under the effective Hamiltonian

H_{eff} can be approximately decomposed as

$$U_0(\alpha) = e^{-i\alpha H_{eff}} \approx U_{control}(\alpha) U_z(\alpha), \quad (7)$$

by generalizing the method in Ref. [33] into general cases with arbitrary controlled rotation on multi-spin

systems, where $U_z(\alpha)$ denotes an additional conditional phase factor. Hence, the propagator of the effective

Hamiltonian of a transition-selective excitation over the duration of the pulse $\tau = \alpha / \Omega_0$ is equivalent to

$U_{control}(\alpha)$ of Eq. (3) up to conditional phases as long as $\Omega_0 \ll 2\pi \min(J_{0i})$. The controlled-NOT gate with

two spins has been detailedly analyzed in Ref.[33]. Fig. 2 shows the numerical simulations of the gate fidelity[33]

$F(U_0, U_2) = |Tr(U_0^\dagger U_2) / N|^2$ for (a) a 3-spin homonuclear system and (b) a 4-spin heteronuclear system

with the carbon-13 labeled alanine of our experimental physical system in different exciting angles α . Here,

$U_2(\alpha) = U_{control}(\alpha) U_z(\alpha)$ is the approximate propagator whereas $U_0(\alpha)$ is the exact one under the

effective Hamiltonian H_{eff} . We take a quality factor $Q = 1 - F$. The figure manifests that when $\Omega_0 / \pi J_{01}$

is small enough (e.g., < 0.4), the gate fidelities can reach above the order of 0.99, e.g., for the

transition-selective pulse employed in our experiment, $\Omega_0 / \pi J_{01} \approx 0.179$ for $\tau = 80ms$ and its gate fidelity

$F(U_0, U_2) \approx 0.999$. It can be seen from fig. 2 that the gate fidelities of a 4-spin system are higher than that of

a 3-spin system as a result of the fact $J_{03} > J_{01}, J_{02}$ in the alanine molecule. In addition, in the preparation

procedure of the labeled PPS, the transition-selective excitation is applied on such an initial state $\rho_0 = I_{0z}$, so

that $\rho = U_2(\alpha) I_{0z} U_2^\dagger(\alpha) = U_{control}(\alpha) I_{0z} U_{control}^\dagger(\alpha)$ because the phase factor $U_z(\alpha)$ commutes with

I_{0z} . Hereby, the effects of the conditional phases are cancelled out and the transition-selective pulse to

implement the controlled- R_{0y} gate in Fig. 1(a) is efficient and reliable in our experiment.

The labeled PPS $I_{0z} I_1^\alpha I_2^\alpha I_3^\alpha$ obtained experimentally by applying the pulse sequence in Fig. 1(b) is

shown in Fig. 3, along with the reference spectrum of C^α . It can be seen from Fig. 3 (b) that only one transition

of spin I_0 corresponding to $I_1^\alpha I_2^\alpha I_3^\alpha (|000\rangle\langle 000|)$ is retained, indicating that the computational qubits were successfully prepared into the logic state $|000\rangle$. Meanwhile, by a comparison of two spectral signals in Fig. 3, the signal intensity of the labeled PPS was reduced to about 80%. To roughly estimate the intensity decay of the observer spin during the transition-selective pulse [34], we got $M(t)/M(0) = e^{-t/T_2} = 0.82$ where T_2 the spin-spin relaxation time of spin I_0 which is measured to be 0.41ms, $M(0)$ the intensity of the spin at the beginning of the operation and $M(t)$ the final intensity after the excitation. Because of the high fidelity of the transition-selective pulse theoretically, the main cause for the signal decay during the preparation of the labeled PPS is the relaxation effect of the low-power, long-duration transition-selective pulse. Besides, the sources of experimental errors are also due to inhomogeneity of RF fields and static magnetic fields, the imperfections of the spin- and transition-selective excitations, etc.

III. NMR SPECTRAL IMPLEMENTATION OF BERNSTEIN-VAZIRANI'S ALGORITHM

Bernstein-Vazirani's (B-V) problem [11] can be expressed as follows: Suppose that a black box *oracle* computes a function $f : \{0,1\}^n \rightarrow \{0,1\}$, where $f_a(x) = a \bullet x = (a_1 \wedge x_1) \oplus (a_2 \wedge x_2) \oplus \dots \oplus (a_n \wedge x_n)$, and $a, x \in \{0,1\}^n$, a_i and x_i are the i th qubits of a and x , and consider the goal of determining a . Classically, it would require n queries of the *oracle* to determine a with certainty. In 1993, Bernstein and Vazirani [11] first gave a quantum algorithm to solve this problem with two queries, which was slightly improved to comprise a single query [35,36]. The scheme for B-V algorithm [35] is illustrated in Fig. 4. The quantum *oracle* is enacted by a unitary operation U_f on the computational basis

$$U_f : |x\rangle|y\rangle \rightarrow |x\rangle|y \oplus f(x)\rangle, \quad (8)$$

where $|x\rangle$ is the database register, \oplus denotes addition modulo 2, and a single qubit $|y\rangle$ is the oracle qubit.

The whole procedure can be described as:

$$\begin{aligned} & |0\rangle^n \otimes \frac{|0\rangle - |1\rangle}{\sqrt{2}} \xrightarrow{H^{(n)}} \frac{1}{\sqrt{2^n}} \sum_{x=0}^{2^n-1} |x\rangle \otimes \frac{|0\rangle - |1\rangle}{\sqrt{2}} \\ & \xrightarrow{U_f} \frac{1}{\sqrt{2^n}} \sum_{x=0}^{2^n-1} (-1)^{a \bullet x} |x\rangle \otimes \frac{|0\rangle - |1\rangle}{\sqrt{2}} \\ & \xrightarrow{H^{(n)}} \frac{1}{\sqrt{2^n}} \sum_{x,y=0}^{2^n-1} (-1)^{x \bullet (a \oplus y)} |y\rangle \otimes \frac{|0\rangle - |1\rangle}{\sqrt{2}} \equiv |a\rangle \otimes \frac{|0\rangle - |1\rangle}{\sqrt{2}}. \end{aligned} \quad (9)$$

Measuring the n -qubit database register yields the value of a with probability one. Eq. (9) implies that there is no entanglement between the database register and the oracle qubit. Notice that the state of the oracle qubit is itself not changed throughout the quantum algorithm, only used to change the phase of the state $|x\rangle$ according to the parity of the function $f_a = a \bullet x$ when querying the black box. Hence, it is completely redundant [36,37] and can be removed by redesigning the oracle as an n -qubit unitary transformation U_a [37],

$$U_a : |x\rangle \rightarrow (-1)^{a \bullet x} |x\rangle, \quad (10)$$

instead of the $n+1$ -qubit unitary transformation U_f . U_a can be decomposed as direct products of single qubit operators $U_a = U^1 \otimes U^2 \otimes \dots \otimes U^n$, where $U^i = \begin{cases} E_i, & a_i = 0 \\ \sigma_{iz}, & a_i = 1 \end{cases}$. Obviously, U_a cannot create entanglement among the database qubits, which is the most remarkable property [34] that there is no entanglement in both the refined and the original B-V algorithm (see Eq. (9)) at any timestep! Unlike the refined Deutsch-Jozsa algorithm, the entanglement is possible when $n > 2$ depending on the form of the function f [37]. Nevertheless, without entanglement B-V algorithm reduces the number of queries required classically from n to 1, which demonstrates that quantum-over-classical improvement can be achieved with the help of *quantum parallelism* [36]. However, the further exponential speed-up in quantum algorithms relies upon *the utilization of entanglement* as the essential non-classical feature, such as Shor's algorithm, which provides the full power of quantum computation[39].

For the labeled PPS $I_{0z} I_1^\alpha I_2^\alpha \dots I_n^\alpha$, the algorithm is applied to the computational qubits I_1, I_2, \dots, I_n , while the observer spin I_0 is not directly involved in the quantum computation. Thereby, after a spin-selective read-out pulse $(\pi/2)_y^0$, one can detect the magnetization of spin I_0 [29]

$$\begin{aligned} M_0 &= \text{Tr} \left[I_0^+ \left(I_{0x} \otimes U_{BV} \left(I_1^\alpha I_2^\alpha \dots I_n^\alpha \right) U_{BV}^\dagger \right) \right] \\ &= \text{Tr} \left[I_0^+ \left(I_{0x} \otimes \rho_{out} \right) \right] = \rho_{11} + \rho_{22} + \dots + \rho_{nn}, \end{aligned} \quad (11)$$

where $I_0^+ = I_{0x} + iI_{0y}$ and ρ_{ii} related to the database $|i-1\rangle$ ($i = 1, 2, \dots, N = 2^n$) indicates the i th diagonal element of the output density matrix $\rho_{out} = U_{BV} \left(I_1^\alpha I_2^\alpha \dots I_n^\alpha \right) U_{BV}^\dagger$ with $U_{BV} = H^{(n)} U_a H^{(n)}$, corresponding to each of 2^n individual spectral resonance lines in the NMR spectrum of the observer spin I_0 , respectively. If all

of $J_{0i} > 0$, ρ_{11} is the transition at the lowest frequency and ρ_{NN} , the one at the highest frequency as illustrated in Fig. 3 (a). That is, the results of projective measurements under the computational basis of qubits can be obtained from the split peak positions in the spectra. Theoretically, $\rho_{out} = |a\rangle\langle a|$ for the B-V algorithm denotes that the state of the n computational qubits is in the state $|a\rangle$, i.e., $\rho_{ii} = 1$ for $|i-1\rangle = |a\rangle$ while $\rho_{ii} = 0$ for $|i-1\rangle \neq |a\rangle$ in Eq. (11). So only the transition line of spin I_0 relevant to the state $|a\rangle$ is retained in the spectrum of spin I_0 . The “answer” of the computation is intuitively identified by the spectrum of spin I_0 . From Eq. (11), we can see that if the “answer” of some computational problems is only related to the information of the diagonal elements of the output density matrix, or the results of projective measurements under the computational basis of qubits are only needed in the algorithms, the read-out of spectroscopical mapping is favorable.

To implement B-V algorithm in NMR, the corresponding pulse sequences should be firstly designed [30]. As E_i represents no pulse; σ_{iz} can be realized by the NMR pulse $(\pi)_z^i \sim (\pi/2)_{-y}^i (\pi)_x^i (\pi/2)_y^i$; Hadamard gate $H_i = \frac{1}{\sqrt{2}} \begin{pmatrix} 1 & 1 \\ 1 & -1 \end{pmatrix}$ by $(\pi)_x^i (\pi/2)_y^i$ or $(\pi/2)_{-y}^i (\pi)_x^i$, the final simplified NMR pulse sequences can be $\prod_i (\pi)_x^{a_i}$, i.e., to apply a π pulse on spin I_i when $a_i = 1$, otherwise no operation. However, the plain conclusion embodies the whole procedure of quantum algorithm. The refined version of B-V algorithm for two qubits has been experimentally implemented on a 2-qubit NMR quantum computer [37]. Applying the reduced pulse sequence of the B-V algorithm to the 3-qubit labeled PPS prepared above, the experimental results of the algorithm are presented in Fig. 5, which are consistent with the theoretical predictions. Detections of all states were achieved by a spin-selective $(\pi/2)_y^0$ pulse, followed by acquisition and Fourier transformation of the signal [29]. The spectrum of spin I_0 carries the results of the quantum computations. Due to the algorithm is implemented by only several spin-selective π pulses on computational qubits, the experimental errors are on the same order with the labeled PPS.

IV. CONCLUSION

In summary, by introducing the model of quantum circuit into the preparation of the labeled PPS, we have experimentally implemented a method of preparing labeled pseudo-pure states by the multiplet-component

excitation with a 4-qubit NMR quantum processor. The controlled-rotation gate is of central importance in quantum computing. We choose the direct implementation of the transition-selective scheme, and by theoretically analyzing the entire Hamiltonian of the system, a transition-selective pulse can yields a controlled-rotation gate up to phase factors with high fidelity when $\Omega_0 \ll 2\pi \min |J_{0i}|$, especially for the present preparation scheme of a labeled PPS. In some sense, the simple implementation might be more efficient than the serial implementation. But the long-duration transition-selective excitation greatly causes the signal decay due to relaxation effects and the demanding requirement for the sample choice that needs all lines to be well-resolved. Moreover, based on “spectral implementation”, a 3-qubit Bernstein-Vazirani’s algorithm has been experimentally demonstrated on such a labeled PPS. In the spectrum of spin I_0 detected at the end of experiments, the label of the highest peak gives the same answer as the projective measurement under the computational basis of qubits, which is good agreement with theory. The introduction of the observer spin I_0 provides a convenient way to read out the results of the computation efficiently and reliably for certain specific computational problems.

ACKNOWLEDGMENTS

We would like to thank Xiaodong Yang, Hanzeng Yuan, and Xu Zhang for help in the course of experiments. This work is supported by the National Fundamental Research Program (2001CB309300).

Appendix A DECOMPOSITION OF THE WHOLE PROGAGATOR FOR A SINGLE-TRANSITION EXCITATION

For a transition-selective excitation, a basic requirement in experiment is $\left| \frac{\gamma_0}{2\pi} \mathbf{B}_1 \right| < \left| \min (J_{0i}) \right|$, thus the off-resonance effects due to the I_{iy} terms in H_{eff} of Eq. (6) can be ignored in a weak-coupled system [33].

Consequently, we deal with $H_{eff}^0 = H_{eff} - \sum_{k=1}^n \Omega_k I_{ky}$ instead of H_{eff} with a very good approximation.

Consider a 3-spin system and let

$$a_i = \frac{\omega_0 - \omega_i}{\Omega_0}, \quad b_i = \frac{\pi J_{0i}}{\Omega_0} \quad \text{and} \quad c_1 = \frac{\pi J_{12}}{\Omega_0} \quad (i = 1, 2). \quad (\text{A.1})$$

One gets from Eq. (6)

$$H_{eff}^0 / \Omega_0 \Big|_{n=2} = P + Q_{--} I_1^\beta I_2^\beta + Q_{+-} I_1^\alpha I_2^\beta + Q_{-+} I_1^\beta I_2^\alpha + Q_{++} I_1^\alpha I_2^\alpha \quad (A.2)$$

where

$$\begin{aligned} P &= \sum_{i=1}^2 (a_i - b_1 - b_2) I_{i_z} + 2c_1 I_{1_z} I_{2_z}, \\ Q_{--} &= -2(b_1 + b_2) I_{0_z} + I_{0_y}, \\ Q_{-+} &= -2b_1 I_{0_z} + I_{0_y} \\ Q_{+-} &= -2b_2 I_{0_z} + I_{0_y}, \\ Q_{++} &= I_{0_y}. \end{aligned} \quad (A.3)$$

Note that the last four terms in Eq. (A.2) commute each other. P is a diagonal matrix and $H_{tm} = Q_{++} I_1^\alpha I_2^\alpha$.

However, $Q_{--} I_1^\beta I_2^\beta, Q_{-+} I_1^\beta I_2^\alpha$ and $Q_{+-} I_1^\alpha I_2^\beta$ are not diagonal and can be readily diagonalized [33] since

$$Q_{--} = -e^{i\theta_1 I_{0_x}} I_{0_z} e^{-i\theta_1 I_{0_x}} \sqrt{1 + 4(b_1 + b_2)^2}, \theta_1 = \arctan(1/(2b_1 + 2b_2)), \quad (A.4)$$

and the similar expressions for Q_{-+} with $\theta_2 = \arctan(1/(2b_1))$ and Q_{+-} with $\theta_3 = \arctan(1/(2b_2))$.

Therefore, we can evaluate the difference between two unitary propagators without and with this

transformation $U_T = e^{i\theta_3 I_{0_x} I_1^\alpha I_2^\beta} e^{i\theta_2 I_{0_x} I_1^\beta I_2^\alpha} e^{i\theta_1 I_{0_x} I_1^\beta I_2^\beta}$, i.e., $U_1 = e^{-i\alpha H_{eff}^0}$ and $U_2 = U_T^\dagger U_1 U_T$ by calculating the

gate fidelity between U_1 and U_2 , which can be defined by

$$\begin{aligned} F(U_1, U_2) &= \left| \text{Tr}(U_1^\dagger U_2) / N \right|^2 \\ &= \left| \text{Tr} \left(e^{i\alpha Q_{--} I_1^\beta I_2^\beta} e^{i\alpha Q_{-+} I_1^\beta I_2^\alpha} e^{i\alpha Q_{+-} I_1^\alpha I_2^\beta} \bullet e^{i\alpha \sqrt{1+4(b_1+b_2)^2} I_{0_z} I_1^\beta I_2^\beta} e^{i\alpha \sqrt{1+4b_2^2} I_{0_z} I_1^\alpha I_2^\beta} e^{-i\alpha \sqrt{1+4b_1^2} I_{0_z} I_1^\beta I_2^\alpha} \right) / 8 \right|^2 \\ &= \left| 1 - \frac{1}{2^2} \left[\sin^2 \left(\frac{\alpha}{2} \sqrt{1+4(b_1+b_2)^2} \right) \left(1 - \frac{2(b_1+b_2)}{\sqrt{1+4(b_1+b_2)^2}} \right) + \sin^2 \left(\frac{\alpha}{2} \sqrt{1+4b_2^2} \right) \left(1 - \frac{2b_2}{\sqrt{1+4b_2^2}} \right) + \sin^2 \left(\frac{\alpha}{2} \sqrt{1+4b_1^2} \right) \left(1 - \frac{2b_1}{\sqrt{1+4b_1^2}} \right) \right] \right|^2, \end{aligned} \quad (A.5)$$

where N is the dimension of the Hilbert space. In the square bracket, the second factor of each term is much less

than 1 if $\Omega_0 \ll 2\pi \min(J_{01}, J_{02})$, e.g., $1 - \frac{2b_1}{\sqrt{1+4b_1^2}} \leq \frac{1}{4b_1^2} = \frac{\Omega_0}{4(\pi J_{01})^2} \ll 1$ so that $F(U_1, U_2) \rightarrow 1$. Then it

follows that

$$e^{-i\alpha H_{eff}} \approx e^{-i\alpha H_{eff}^0} \approx U_{control}(\alpha) U_z(\alpha) \quad (A.6)$$

with

$$U_z(\alpha) = e^{-i\alpha P} e^{i\alpha\sqrt{1+4(b_1+b_2)^2}I_{0z}I_1^\beta I_2^\beta} e^{i\alpha\sqrt{1+4b_2^2}I_{0z}I_1^\alpha I_2^\beta} e^{-i\alpha\sqrt{1+4b_1^2}I_{0z}I_1^\beta I_2^\alpha}. \quad (\text{A.7})$$

Here, $U_{\text{control}}(\alpha) = e^{-i\alpha H_{\text{int}}}$ is equal to Eq. (3). Hence, the propagator of the effective Hamiltonian of a transition-selective excitation is equivalent to $U_{\text{control}}(\alpha)$ of Eq. (3) up to a conditional phase factor $U_z(\alpha)$. For any n-spin system, the propagator has approximately the analogous decomposition, i.e., except for the transition component irradiated, additional phase factors are yielded for other components of this spin and other spins if $\Omega_0 \ll 2\pi \min(J_{0i})$. In a two-spin system, the exact controlled-rotation gate can be implemented at certain specific power levels, i.e., $F(U_1, U_2) = 1$ for certain specific power levels, while for $n > 2$, $F(U_1, U_2) \rightarrow 1$ at high enough precision.

REFERENCES

- [1] C. H. Bennett and D. P. DiVincenzo, *Nature* 377, 389 (1998).
- [2] C. H. Bennett and P. W. Shor, *IEEE Trans. Inf. Theory* 44, 2724 (1998).
- [3] D. P. DiVincenzo, *Science* 270, 255 (1995).
- [4] M. A. Nielsen and I. L. Chuang, *Quantum Computation and Quantum Information* (Cambridge Univ. Press, Cambridge, 2000).
- [5] P. Shor, Algorithms for quantum computation: discrete logarithms and factoring. *proc. 35th Annu. Symp. on Found. of Computer Science*, (IEEE comp. Soc. Press, Los Alamos, CA. 1994) 124-134.
- [6] J. Preskill, <http://www.theory.caltech.edu/~preskill/ph229>.
- [7] L. K. Grover, *Phys. Rev. Lett.* 79, 325 (1997).
- [8] D. Deutsch, *Proc. R. Soc. Lond. A* 400, 97 (1985).
- [9] D. Deutsch and R. Jozsa, *Proc. R. Soc. Lond. A* 439, 553 (1992).
- [10] D. Simon, *Proc. of 35th Annual Symposium on the Foundations of Computer Science*, p. 116 (1994). Los Alamitos, CA: IEEE Computer Society. (Extended abstract. Full version in 1997 *SIAM J. Comput.* 26.)
- [11] E. Bernstein and U. Vazirani, *Proc. 25th Ann. ACM Symp. on the Theory of Computer* p. 11-20. New York; AM Press, (1993).
- [12] I. L. Chuang, L. M. K. Vandersypen, X. Zhou, D. W. Leung, S. Lloyd, *Nature* 393, 143 (1998); J. A. Jones and Mosca, *J. Chem. Phys.* 109, 1648 (1998); N. Linden, H. Barjat and R. Freeman, *Chem. Phys. Lett.* 296,

- 61 (1998); J. Kim, J.-S. Lee, S. Lee and C. Cheong, Phys. Rev. A 62, 022312 (2000); D. Collins, K. W. Kim, W. C. Holton, H. Sierzputowska-Gracz, and E. O. Stejskal, *ibid.* 62, 022304 (2000); R. Marx, A. F. Fahmy, J. M. Myers, W. Bermel and S. J. Glaser, *ibid.* 62, 012310 (2000); I. L. Chuang, N. Gershenfeld and M. Kubinec, Phys. Rev. Lett. 80, 3408 (1998); J. A. Jones, M. Mosca and R. H. Hansen, Nature 393, 344 (1998); L. M. K. Vandersypen et al., Appl. Phys. Lett. 76, 646 (2000); E. Knill, R. Laflamme, R. Martinez and C.-H. Tsieng, Nature 404, 368 (2000); L. M. K. Vandersypen, M. Steffen, G. Breyta, C. S. Yannoni, R. Cleve and I. L. Chuang, Phys. Rev. Lett. 85, 5452 (2000).
- [13] L. M. K. Vandersypen, M. Steffen, G. Breyta, C. S. Yannoni, M. H. Sherwood and I. L. Chuang, Nature 414, 883 (2001).
- [14] S. Gulde, M. Riebe, G. P. T. Lancaster, C. Becher, J. Eschner, H. Haffner, F. Schmidt-Kaler, I. L. Chuang and R. Blatt, Nature 421, 48, (2003); F. Mintert and C. Wunderlich, Phys. Rev. Lett. 87, 257904 (2001).
- [15] Z. L. Madi, R. Bruschweiler and R. R. Ernst, J. Chem. Phys. 109, 10603 (1998).
- [16] E. Knill, R. Laflamme, R. Martinez and C.-H. Tsieng, Nature 404, 368 (2000).
- [17] R. Laflamme, E. Knill, D. G. Cory, E. M. Fortunato, T. Havel, C. Miquel, R. Martinez, C. Negrevergne, G. Ortiz, M. A. Pravia, Y. Sharf, S. Sinha, R. Somma and L. Viola, quant-ph/0207172.
- [18] D. G. Cory, M. D. Price, W. Maas, E. Knill, R. Laflamme, W. H. Zurek, T. F. Havel, and S. S. Somaroo, Phys. Rev. Lett. 81, 2152 (1998); E. Knill, R. Laflamme, R. Martinez, and C. Negrevergne, Phys. Rev. Lett. 86, 5811 (2001).
- [19] D. G. Cory, A. F. Fahmy and T. F. Havel, Proc. Natl. Acad. Sci. USA 94, 1634 (1997).
- [20] D. G. Cory, M. D. Price and T. F. Havel, Physica D 120, 82 (1998).
- [21] X. Peng, X. Zhu, X. Fang, M. Feng, K. Gao, X. Yang and M. Liu, Chem. Phys. Lett. 340, 509 (2001).
- [22] E. Knill, I. Chuang and R. Laflamme, Phys. Rev. A 57, 3348 (1998).
- [23] L. M. K. Vandersypen, M. Steffen, G. Breyta, C. S. Yannoni, R. Cleve and I. L. Chuang, Phys. Rev. Lett. 85, 5452 (2000).
- [24] N. A. Gershenfeld and I. L. Chuang, Science 275, 350 (1997).
- [25] I. L. Chuang, N. Gershenfeld, M. Kubinec and D. Leung, Proc. Roy. Soc. Lond A 454, 447 (1998).
- [26] J. Kim, J.-S. Lee and S. Lee, Phys. Rev. A 61, 032312 (2000).
- [27] Y. Sharf, T. F. Havel, and D. G. Cory, Phys. Rev. A 62, 052314 (2000)
- [28] U. Sakaguchi, H. Ozawa, C. Amano, and T. Fukumi, Phys. Rev. A 60, 1906 (1999).
- [29] R. Ernst, G. Bodenhausen and A. Wokaun, Principles of Nuclear Magnetic Resonance in One and Two

Dimensions (Oxford Univ. Press, Oxford, 1990).

[30] J. A. Jones, NMR quantum computation. *Prog. NMR Spectrosc.* 38, 325 (2001).

[31] M. D. Price, S. S. Somaroo, A. E. Dunlop, T. F. Havel, and D. G. Cory, *Phys. Rev. A* 60, 2777 (1999); N. Linden, B. Herver, R. J. Carvajo and R. Freeman, *Chem. Phys. Lett.* 311, 321 (1999); N. Linden, B. Herver, R. J. Carvajo and R. Freeman, *Chem. Phys. Lett.* 305, 28 (1999); D. W. Leung, I. L. Chuang, F. Yamaguchi and Y. Yamamoto, *Phys. Rev. A* 61, 042310 (2002); J. A. Jones and E. Knill, *J. Magn. Reson.* 141, 322 (1999).

[32] K. Dorai and D. Suter, quant-ph/0211030.

[33] D. G. Cory, A. E. Dunlop, T. F. Havel, S. S. Somaroo and W. Zhang, quant-ph/9809045.

[34] V. V. Krishna, *Phys. Lett. A* 291, 27 (2001).

[35] R. Cleve, A. Ekert, C. Macchiavello and M. Mosca, *Proc. R. Soc. Lond. A* 454, 339-354, (1998).

[36] D. A. Meyer, *Phys. Rev. Lett.* 85, 2014 (2000).

[37] D. Collins, K. W. Kim, and W. C. Holton, *phys. Rev. A* 58, R1633 (1998).

[38] J. Du, M. Shi, X. Zhou, Y. Fan, B. Ye, and R. Han, *Phys. Rev. A* 64, 042306 (2001).

[39] R. Josza, "Entanglement and quantum computation" in S. A. Huggett, L. J. Mason, K. P. Tod, S. T. Tsou and N. M. J. Woodhouse, eds., *The Geometric Universe: Science, Geometry, and the Work of Roger Penrose* (Oxford:Oxford University Press 1998) 369-379; A. Ekert and R. Jozsa, *Phil. Trans. Roy. Soc. Lond. A* 356, 1769 (1998).

Table 1 Measured NMR parameters for alanine on a Bruker ARX500 spectrometer

spin	ν/Hz	J_C/Hz	J_{C^α}/Hz	J_{C^β}/Hz	J_H/Hz
C' (1)	-4320		34.94	-1.2	5.5
C^α (0)	0	34.94		53.81	143.21
C^β (2)	15793	-1.2	53.81		5.1
H (3)	1550	5.5	143.21	5.1	

FIGURE CAPTIONS

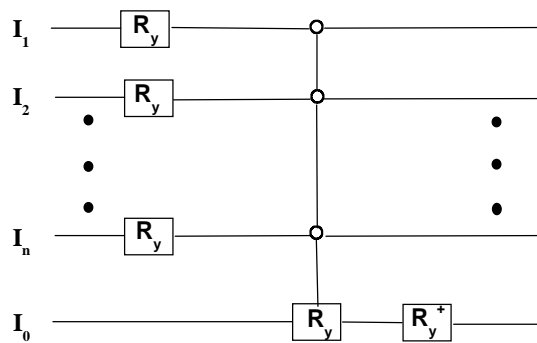
Fig. 1 Quantum circuit (a) and pulse sequence (b) for creating the labeled PPS $I_{0z}I_1^\alpha I_2^\alpha \dots I_n^\alpha$ from thermal equilibrium. The controlled- R_{0y} gate is performed conditional on all computational qubits I_1, I_2, \dots, I_n being in the $|0\rangle$ state represented by open circles. R_y and R_y^\dagger are described in the text. The first $\pi/2$ pulse is applied on all computational qubits I_1, I_2, \dots, I_n and the second $\pi/2$ pulse (denoted by the arc) represents the transition-selective excitation on a single transition of the observer spin I_0 . The pulsed-field gradients (G_z) destroy all transverse magnetization.

Fig. 2 The numerical simulations of the quality factor of gate $Q = 1 - F(U_0, U_2)$ in (a) a 3-spin homonuclear system and (b) a 4-spin heteronuclear system with the alanine molecule in different angles $\alpha = \pi/2$ (denoted by the dotted line) and π (denoted by the solid line). U_0 and U_2 are described in the text.

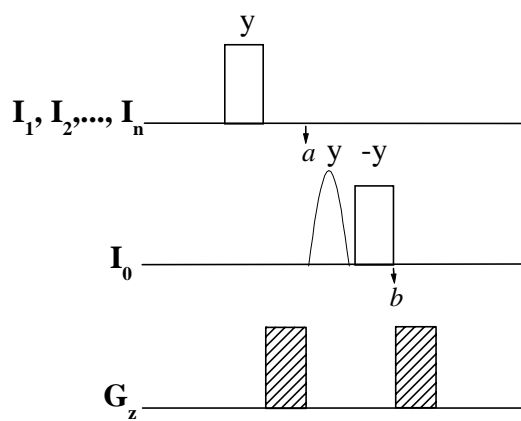
Fig. 3 Experimental spectra (in arbitrary units) for (a) the reference spectrum in thermal equilibrium and (b) the labeled PPS $I_{0z}I_1^\alpha I_2^\alpha \dots I_n^\alpha$. All spectra were obtained by a spin-selective $(\pi/2)_y^0$ pulse on the observer spin I_0 .

Fig. 4 Quantum circuit for B-V algorithm. H represents the Hadamard gate. The unitary operation U_f in the dashed box represents a black box query, which can be simplified as another unitary transformation U_a in the practical experiment (see the text).

Fig. 5 Experimental spectra of implementing the quantum algorithm to solve B-V problem for: (a) $a = 000$ (b) $a = 001$ (c) $a = 010$ (d) $a = 011$ (e) $a = 100$ (f) $a = 101$ (g) $a = 110$ (h) $a = 111$.



(a)



(b)

Fig. 1

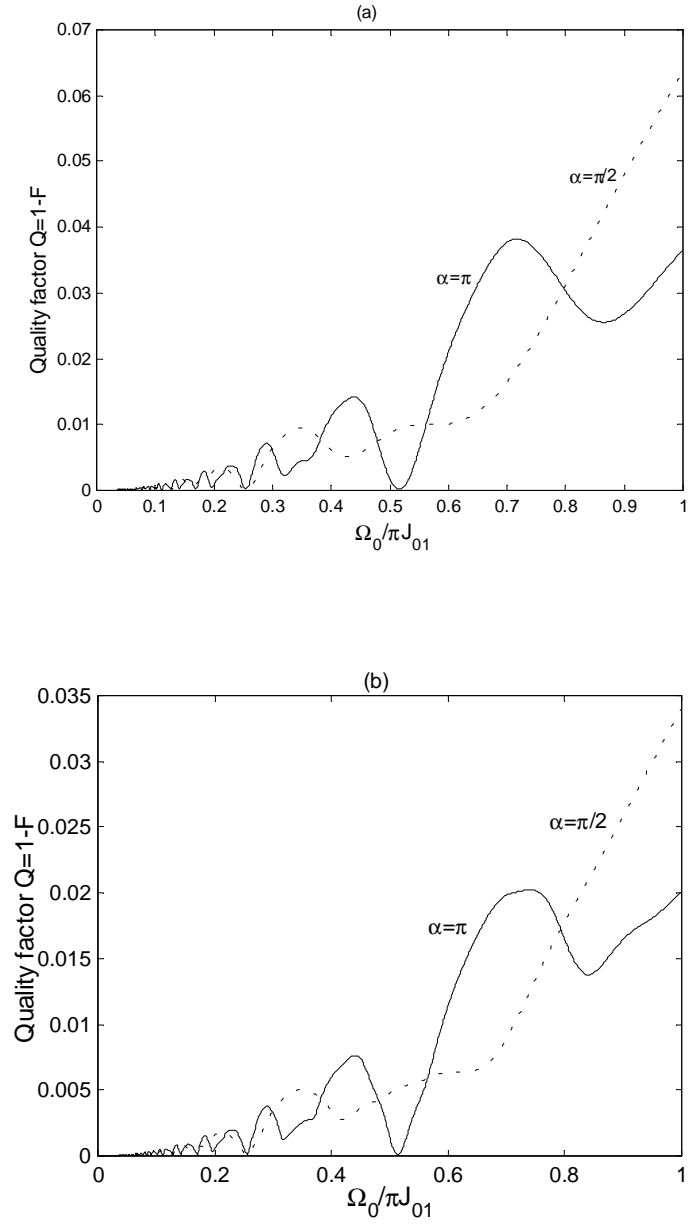


Fig. 2

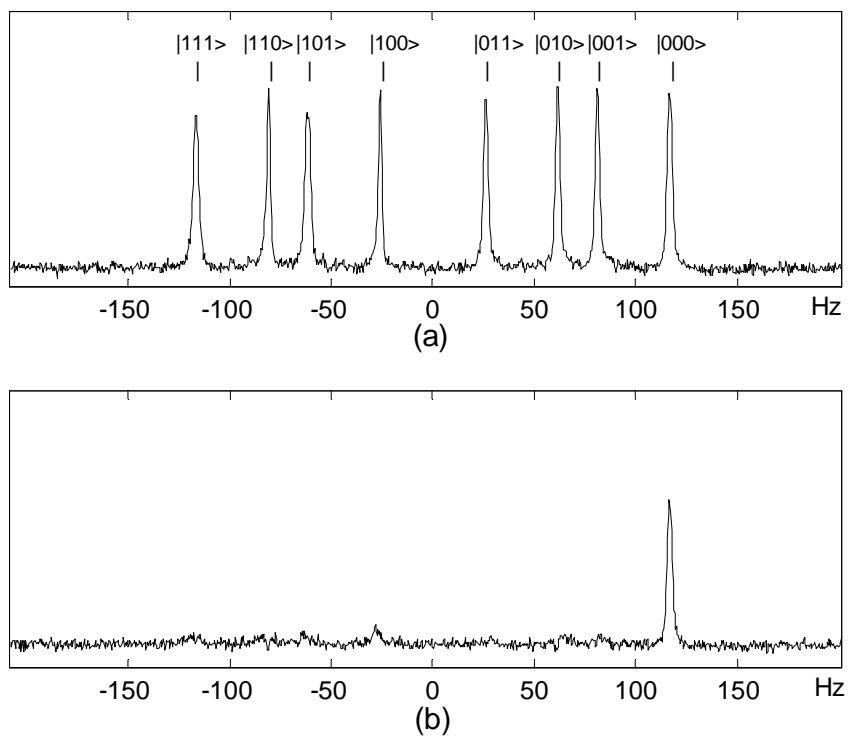


Fig. 3

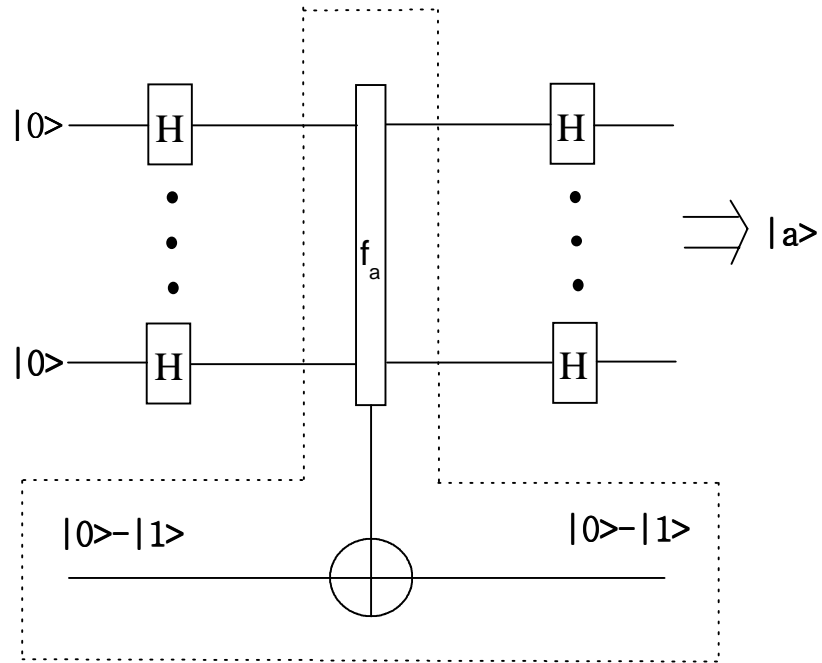


Fig. 4

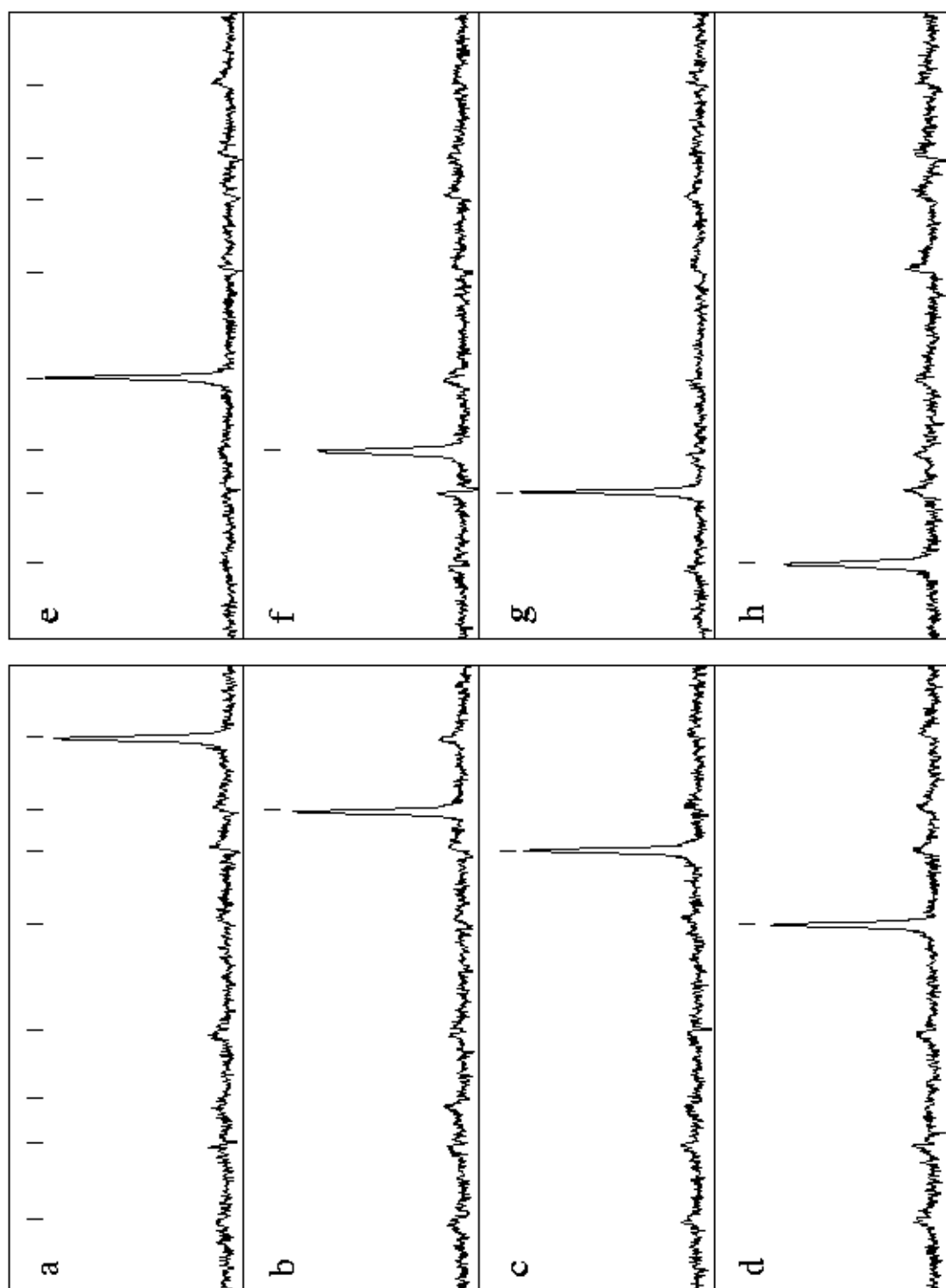


Fig. 5